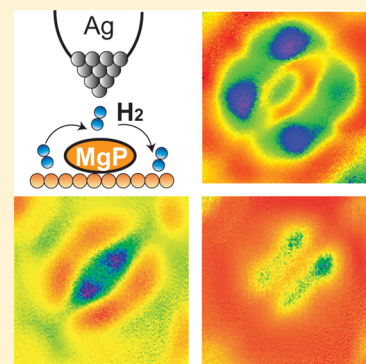


Single-Molecule Rotational and Vibrational Spectroscopy and Microscopy with the Scanning Tunneling Microscope

Arthur Yu,[†] Shaowei Li,[†] Gregory Czap,[†] and W. Ho^{*,†,‡}[†]Department of Physics and Astronomy, University of California, 4129 Frederick Reines Hall, Irvine, California 92697-4575, United States[‡]Department of Chemistry, University of California, 1102 Natural Sciences 2, Irvine, California 92697-2025, United States

ABSTRACT: A new method of imaging with the scanning tunneling microscope (STM) is used to study magnesium porphyrin (MgP) molecules adsorbed on Au(110) surface. Hydrogen molecules are deposited onto the surface and diffuse freely until temporarily trapped in the tunnel junction. The vibrational and rotational modes of the H₂ are monitored with inelastic electron tunneling spectroscopy with the STM. The MgP presents the H₂ with a highly localized position-dependent adsorption potential, which causes variations in the energies of both vibrational and rotational modes of the trapped H₂ molecule. Imaging at the vibrational and rotational energies of H₂ reveals salient features in the chemical structure of the MgP molecule, in particular, the positions of the nitrogen atoms. The electrostatic interaction between H₂ and MgP plays a crucial role in determining the imaged features, which provide a visualization of the interaction potential within the MgP molecule.



1. INTRODUCTION

Since its invention, the scanning tunneling microscope (STM) has become a powerful tool for investigating atomic scale phenomena with unparalleled spatial resolution. It has been used to study surface structure,¹ single-molecule chemistry,² and nanostructures by atomic manipulation.³ Despite these successes, a steady goal has been to extend the chemical and structural sensitivities of the STM. Because STM derives its spatial resolution from sensitivity of the tunneling current to tip–sample distance and local electron density of states, STM topography images rarely replicate molecular structure in detail. As such, chemical identification from STM topography with a bare metal tip is nearly impossible. Over the years, various efforts have been made to develop new techniques for the STM to overcome these challenges. The advent of inelastic electron tunneling spectroscopy (IETS) with the STM partly alleviated the problem of chemical identification, as molecules and complexes can be identified by their vibrational signatures.⁴ While atomic scale resolution is achieved, selected vibrational modes are observed, requiring theoretical analyses of the inelastic tunneling cross sections, and selection rules are distinct for STM-IETS.^{5,6}

More recently, developments in noncontact atomic force microscopy (NC-AFM),⁷ scanning tunneling hydrogen microscopy (STHM),⁸ and inelastic tunneling probe (itProbe)⁹ have provided the possibility to image chemical structures of molecules with unprecedented detail. In all of the above techniques, a “functionalized” tip with a probe molecule is necessary, such as a CO molecule bonded to the tip or a H₂ trapped in the tunnel junction. In general, the interaction between a molecule adsorbed on the surface and the probe molecule causes changes in the probe molecule, which can be

detected as a change in tunneling current in the STM or resonant frequency of the AFM. This interaction must depend sensitively on the relative positions of the adsorbed and probe molecules, giving the techniques their spatial resolution. Using the same basic principle, here we introduce a new method for imaging with the STM that allows for resolution of the internal features of an adsorbed magnesium porphyrin (MgP) molecule on the Au(110) 2 × 1 reconstructed surface. This technique, based on the rotational excitation of H₂, offers new insights into the interactions between the MgP and H₂ molecule and extends the capability of H₂ to act as a sensor of its local chemical environment.

The rotational excitations of H₂ molecules weakly adsorbed on surfaces of metal and decoupling layers have been measured with the STM.^{10,11} It was also shown that changes in the adsorption potential well induced by varying the tip–sample distance shift the energies of both vibrational and rotational modes for the hydrogen temporarily trapped in the tunnel junction.¹⁰ In this respect, the vibrational and rotational modes of H₂ behave similarly to vibrations of a CO molecule attached to the tip.⁹ We can take advantage of the sensitivity of the H₂ modes to their local chemical environment to image the structure of adsorbed molecules in greater detail than is possible with bare metal tip. On the Au(110) 2 × 1 surface, H₂ can diffuse freely and be trapped in the tunnel junction of the STM, even over an adsorbed molecule. While the diffusion rate

Special Issue: Steven J. Sibener Festschrift

Received: January 16, 2015

Revised: February 26, 2015

Published: March 5, 2015

of the H_2 molecules in and out of the tunnel junction is much faster than the imaging time, each H_2 feels the same chemical environment. The MgP molecule is ideal for STM studies due to its nearly planar geometry. In addition, the presence of nitrogen atoms and the central magnesium atom presents a diverse chemical environment to the trapped H_2 molecule, so the interaction between the H_2 and different chemical components can be probed within a single adsorbed molecule.

2. EXPERIMENT

The experiment was performed in a home-built STM system operating at temperature of 10 K and base pressure of 3×10^{-11} Torr.¹² The Au(110) 2×1 surface was prepared by repeated cycles of Ne^+ sputtering and annealing to 680 K. The STM tips were electrochemically etched from high-purity Ag wires. Upon lowering the temperature to 10 K, MgP molecules were thermally evaporated onto the surface. The H_2 gas was introduced into the chamber at a pressure of 1×10^{-10} Torr for at least 5 min. CO molecules were also dosed onto the surface, allowing the possibility of transferring a CO molecule to the tip for increasing the imaging resolution.

3. RESULTS AND DISCUSSION

In the absence of H_2 as imaged by the bare metal tip, MgP molecules appear as a two-lobed square protrusion straddling the reconstructed Au rows (Figure 1a). In comparison, the

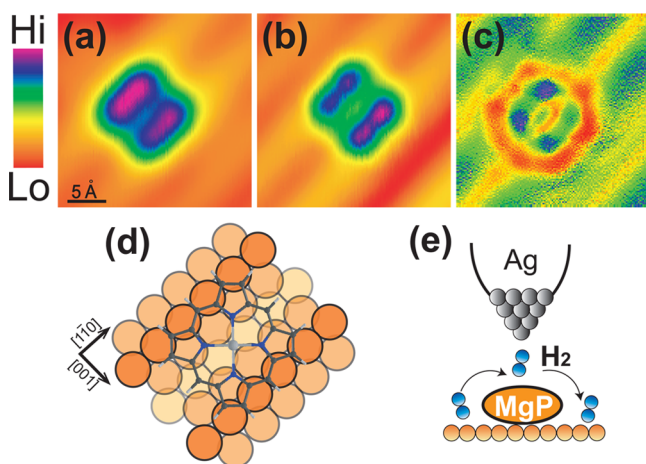


Figure 1. STM topography taken (a) before H_2 exposure, at set point $V_B = 50$ mV, $I_T = 0.1$ nA, (b) with background H_2 , at the same set point, and (c) with CO-terminated tip in H_2 environment, at $V_B = 500$ mV, $I_T = 0.1$ nA. The rows of surface Au atoms are resolved in these topographic images. (d) Adsorption geometry of magnesium porphyrin (MgP) molecule on Au(110) 2×1 reconstructed surface. The first, second, and third atomic layers of the Au surface are depicted by distinct colors with increasing lightness. (e) Schematic of tunneling junction, with a single H_2 diffusing over the MgP molecule and being temporarily trapped in the tunneling junction.

topographic image taken in the presence of H_2 is shown in Figure 1b, and that taken additionally with a CO-terminated tip (in the presence of H_2) is shown in Figure 1c. A schematic diagram of the adsorption site of MgP on Au(110) 2×1 is shown in Figure 1d. After the surface is dosed with H_2 , the H_2 molecules diffuse freely on the Au(110) 2×1 surface with adsorbed MgP molecules (Figure 1e). Because of Pauli repulsion between electrons in the H_2 molecules and in atoms of the substrate, high-resolution images of the substrate

can be obtained when certain conditions are met.^{13,14} In this regime, it is possible to resolve the Au atoms on the surface.¹⁰ Even outside this regime, however, the effect of H_2 can be readily seen in Figure 1b, where the four-lobed symmetry of the MgP is restored.

To investigate the interaction between H_2 and MgP, we performed IETS measurements at different points within the molecule. Figure 2 shows dI/dV (panel a) and d^2I/dV^2 (panel

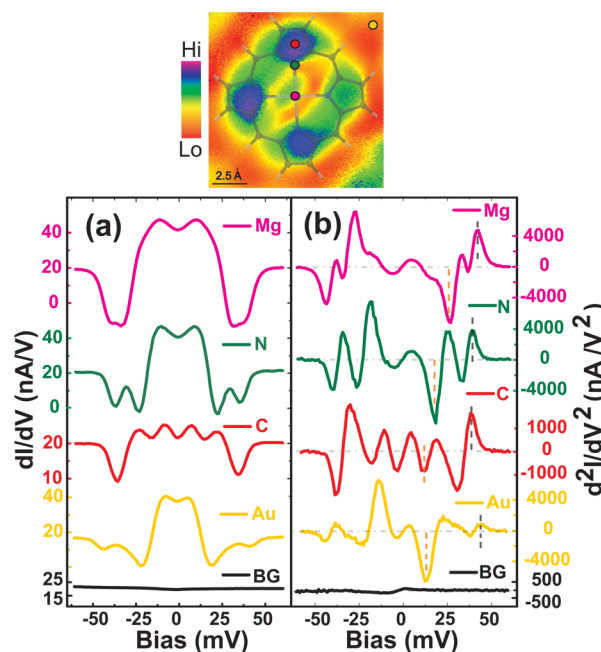


Figure 2. Measurement of (a) dI/dV and (b) d^2I/dV^2 spectra over different points in the molecule. The topographic image at the top was taken with CO-terminated tip and overlaid with a scaled molecular skeletal structure of MgP. The position of the tip for each spectrum is indicated by a color dot in the image. The orange and black dashed lines indicate positions for the vibrational and rotational energies of the H_2 , respectively. The background spectrum was taken over the Au surface in the absence of H_2 . All spectra were taken at a set point of $V_B = 50$ mV, $I_T = 1$ nA from -60 to 60 mV with lock-in modulation at 341 Hz and $V_{rms} = 3$ mV.

b) spectra taken over the central Mg atom, the site of a nitrogen atom, and over the center of the pyrrole ring. To locate these features within the molecule, we took an image with a CO-terminated tip (top of Figure), which shows the outline of molecule. (See also Figure 1c.) In each spectrum, two features are particularly notable: the lower energy dip in d^2I/dV^2 corresponding to the excitation of the vibrational mode with H_2 bouncing against the surface (orange dashed line) and the higher energy peak in d^2I/dV^2 corresponding to excitation of the rotational mode of H_2 (black dashed line). Comparing spectra taken over different locations, it is apparent that both the energy and the relative intensity of these two modes change sensitively with tip position, hence the local chemical environment.

Figure 3 shows IETS spectra taken by positioning the tip at different positions along an axis of the molecule. The dashed lines indicate the positions of the vibrational and rotational energies of H_2 at these different positions over the molecule. As the tip was moved from the outer edge to the center of the molecule, there was an upshift of both the vibrational and rotational energies. Over the Au surface and around the carbon

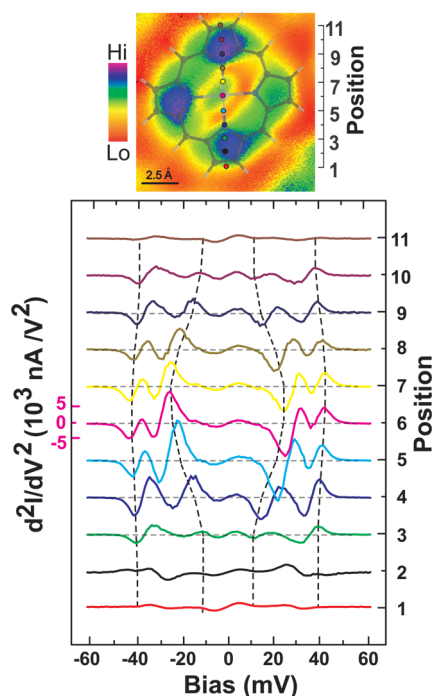


Figure 3. STM-IETS mapping of MgP molecule. d^2I/dV^2 was measured at 11 points along an axis of the MgP (top). The position of each spectrum is indicated by a colored dot on the topographic image, as well as by the number scale on the right side of the image. All spectra were taken with set point $V_B = 50$ mV, $I_T = 1$ nA, bias from -60 to 60 mV, with lock-in modulation at 341 Hz and $V_{rms} = 3$ mV. The two inner dashed lines indicate the energy of the vibrational (bouncing against the surface) mode of the H_2 . The two outer dashed lines indicate the energy of the $j = 0 \rightarrow 2$ rotational excitation of H_2 . The dashed lines are drawn through peak/dip positions on the x axes (the actual energy positions), not through the maxima/minima of the peaks/dips. As the tip moves toward the center of the molecule, both the vibrational and rotational energies shift up.

five-member rings, the vibrational energies are 11 to 12 meV. This mode energy shifts to 19 meV near the nitrogen atoms and to 27 meV over the Mg atom. The rotational energy also shifts but not as significantly. It increases from 38 meV over the carbon rings to 42.5 meV over the Mg atom.

In Figure 4, we performed IETS imaging at different biases. From these images, several interesting features can be seen. In images taken at 13 and 30 mV about the vibrational mode, features emerge that mirror the symmetry of the underlying Au lattice. The two small circular features on two sides of the center in the image at 30 mV, after lateral distance calibration, match with positions of Au atoms underneath, indicating the possible involvement of trough atoms in the bonding between MgP and Au surface. Results from this image were included in the determination of the schematic diagram in Figure 1d. At the rotational energy of 43 meV, we can see four lobes in the image. From a comparison with the calibrated molecular skeleton, these lobes correspond to the positions of the four nitrogen atoms. These features are not clearly resolved or even absent when the imaging bias is off resonance of the rotational peak, as shown for 39 (Figure 4c) and 45 mV (Figure 4e). Interference from the vibrational line shape is absent on the high-energy side of the rotation, and hence the sharpness of rotational imaging is demonstrated by the lack of strong features in Figure 4e. Overall, the d^2I/dV^2 images reveal chemical and structural information on the adsorbed molecule not seen in constant current topography (Figure 4f). These results introduce spectroscopic vibrational and rotational imaging and provide an opportunity to better understand the interaction potentials among H_2 , MgP, and the Au substrate.

In standard theory, the energy of a vibrational mode of a molecule is influenced by the curvature of the interaction potential. The large upshift of the vibrational energy for H_2 toward the center of the MgP suggests that the curvature of the interaction potential is larger near the center of the MgP molecule than near the outer rings. The increase in intensity of the IETS signal near the center could be due to a larger IETS

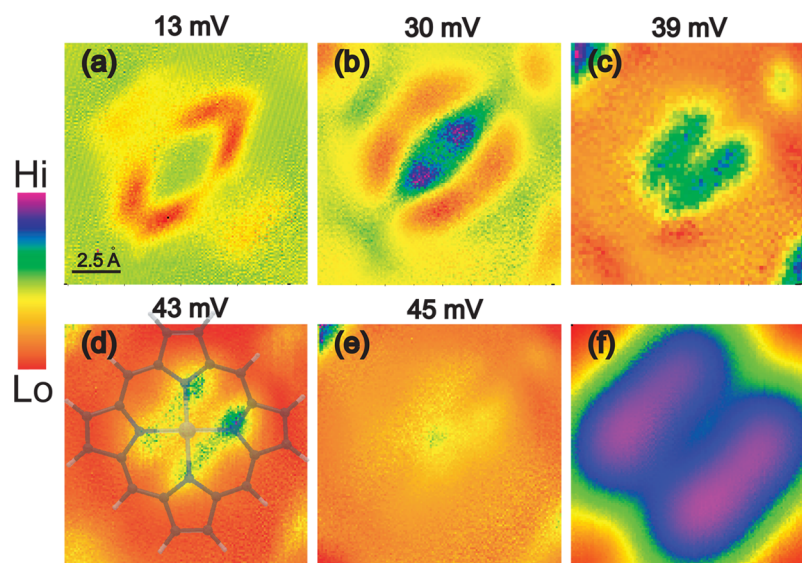


Figure 4. (a–e) IETS imaging of a MgP molecule on the Au(110) 2×1 surface. In all images, the junction was set at $V_B = 50$ mV, $I_T = 1$ nA at each pixel, followed by disabling the feedback, ramping the bias to a chosen voltage, and recording d^2I/dV^2 signal by lock-in technique. The junction was reset at the same set point following lock-in measurement at each pixel. Thus, each image depicts the spatial distribution of the d^2I/dV^2 signal strength at that particular voltage. A scaled model of MgP molecule is overlaid in panel d to show that positions of the lobes in the image correspond to positions of the four nitrogen atoms. (f) For comparison, constant current topographic image taken at set point $V_B = 50$ mV, $I_T = 1$ nA.

cross section and increased trapping time of the H_2 in the tunnel junction. Because only one molecule is in the junction at a time, a rough estimate gives an increase by a factor of 2 in the trapping time, in proportion to the IETS signal intensity. The nature of the changes in the IETS line shape and intensity, however, is beyond the scope of this paper. The presence of substrate features in the IETS imaging (Figure 4b) indicates the important role Au surface atoms play in determining the interaction potential between MgP and H_2 . That should not be a surprise, as in the absence of a decoupling layer, the molecular orbitals of MgP hybridize with the electronic states of the Au substrate. As such, the molecule–substrate interaction can also contribute to increased binding of H_2 to the center of MgP. Similarly, variation in the interaction potential can also transform the geometry (i.e., bond length) of the H_2 , causing a shift in its rotational energy. Figures 2 and 3 indicate that there is a downshift of the rotational energy when H_2 is over the outer rings of the MgP, as compared with over bare Au surface and center of the molecule. The energy shift suggests that the bond length of H_2 is increased over the porphyrin rings.

Because the energies of the vibrational and rotational modes of H_2 depend sensitively on its interaction potential with the MgP, the spatial distribution of these excitations at certain energies reveals details of the potential energy surface. The role of the molecule's different chemical constituents in shaping the interaction potential surface can be investigated through vibrational and rotational microscopy. As we have seen, prominent substrate features in the IETS imaging at 30 mV (Figure 4b) suggest that surface Au atoms play an important role in determining the interaction potential for H_2 . The clear features matching the positions of the four nitrogen atoms in the IETS image at 43 mV (Figure 4d) reveal similarly important contributions from the nitrogen atoms. The effect from the central Mg atom can also be seen by the relatively weak feature in the image at 45 mV (Figure 4e). It is evident that these IETS images at the vibrational and rotational energies provide detailed information about the spatial distribution of the interaction potential between H_2 and the adsorbed molecule, highlighting the effects of the molecule's different chemical constituents in this interaction.

The interaction potential between the trapped H_2 and MgP is mostly dominated by the electrostatic interaction, which gives rise to the high-resolution imaging by NC-AFM and IETS-STM, as recently proposed by Hapala and colleagues.¹⁵ When the tip is close to the surface, the relaxation of the probe molecule in response to the highly localized Pauli repulsion by the surface molecule sharpens the electrostatic features, which closely follow the molecular skeleton. The experiment presented here is in the regime where the STM tip is far away from the substrate such that Pauli repulsion is not significant. If that had not been the case, topography of the MgP molecule would resemble those previously found in the STHM experiments.¹³ In this distant regime, the image is dominated by the probe sample (in this case, H_2 and MgP) electrostatic interaction, resulting in direct resemblance of the image to the Hartree potential. The IETS images from Figure 4 can then be interpreted as the Hartree potential cross sections at various energies.¹⁶ Features associated with the Au atoms in Figure 4b and the N atoms in Figure 4d can be thought of as electronegative centers that preferentially trap the H_2 molecule as reflected in the enhanced signals.

4. CONCLUSIONS

In conclusion, we have shown that vibrational and rotational excitations of H_2 molecules can be used as a probe to image adsorbed molecules in greater structural and chemical detail than possible by topographic imaging. While H_2 IETS imaging cannot resolve features as sensitively as itProbe with CO tip, it still elucidates the structure of the imaged molecule and its interaction with H_2 . Analyses of the images reveal the electrostatic forces that are involved in the interaction between H_2 and MgP. Vibrational and rotational IETS imaging of the H_2 over the adsorbed MgP relates to the Hartree potential of the MgP molecule. Results presented in this paper show the great potential of H_2 IETS imaging as a tool to resolve and visualize the spatial distribution of the interaction potential within an adsorbed molecule.

AUTHOR INFORMATION

Corresponding Author

*E-mail: wilsonho@uci.edu. Tel: (949) 824-5234.

Notes

The authors declare no competing financial interest.

ACKNOWLEDGMENTS

This work is supported by the National Science Foundation Center for Chemical Innovation on Chemistry at the Space-Time Limit (CaSTL) under grant no. CHE-0802913 (A.Y., S.L.) and by the Chemical Sciences, Geosciences, and Biosciences, Office of Basic Energy Science, U.S. Department of Energy under grant no. DE-FG02-06ER15826 (G.C.).

REFERENCES

- (1) Binning, G.; Rohrer, H.; Gerber, C.; Weibel, E. 7×7 Reconstruction on Si(111) Resolved in Real Space. *Phys. Rev. Lett.* **1983**, *50*, 120.
- (2) Ho, W. Single-Molecule Chemistry. *J. Chem. Phys.* **2002**, *117*, 11033.
- (3) Crommie, M. F.; Lutz, C. P.; Eigler, D. M. Confinement of Electrons to Quantum Corrals on a Metal Surface. *Science* **1993**, *262*, 218–220.
- (4) Stipe, B. C.; Rezaei, M. A.; Ho, W. Single Molecule Vibrational Spectroscopy and Microscopy. *Science* **1998**, *280*, 1732–1735.
- (5) Reed, M. Inelastic Electron Tunneling Spectroscopy. *Mater. Today* **2008**, *11*, 46.
- (6) Lorente, N.; Persson, M. Theory of Single Molecule Vibrational Spectroscopy and Microscopy. *Phys. Rev. Lett.* **2000**, *85*, 2997–3000.
- (7) Gross, L.; Mohn, F.; Moll, N.; Liljeroth, P.; Meyer, G. The Chemical Structure of a Molecule Resolved by Atomic Force Microscopy. *Science* **2009**, *325*, 1110–1114.
- (8) Temirov, R.; Soubatch, S.; Neucheva, O.; Lassisse, A. C.; Tautz, F. S. A Novel Method Achieving Ultra-High Geometrical Resolution in Scanning Tunneling Microscopy. *New J. Phys.* **2008**, *10*, 053012.
- (9) Chiang, C. L.; Xu, C.; Han, Z. M.; Ho, W. Real-Space Imaging of Molecular Structure and Chemical Bonding by Single-Molecule Inelastic Tunneling Probe. *Science* **2014**, *344*, 885.
- (10) Li, S. W.; Yu, A.; Toledo, F.; Han, Z. M.; Wang, H.; He, H. Y.; Wu, R. Q.; Ho, W. Rotational and Vibrational Excitations of a Hydrogen Molecule Trapped within a Nanocavity of Tunable Dimension. *Phys. Rev. Lett.* **2013**, *111*, 146102.
- (11) Natterer, F. D.; Patthey, F.; Brune, H. Distinction of Nuclear Spin States with the Scanning Tunneling Microscope. *Phys. Rev. Lett.* **2013**, *111*, 175303.
- (12) Stipe, B. C.; Rezaei, M. A.; Ho, W. A Variable-Temperature Scanning Tunneling Microscope Capable of Single-Molecule Vibrational Spectroscopy. *Rev. Sci. Instrum.* **1999**, *70*, 137–143.

- (13) Weiss, C.; Wagner, C.; Kleimann, C.; Rohlfing, M.; Tautz, F. S.; Temirov, R. Imaging Pauli Repulsion in Scanning Tunneling Microscopy. *Phys. Rev. Lett.* **2010**, *105*, 086103.
- (14) Moll, N.; Gross, L.; Mohn, F.; Curioni, A.; Meyer, G. The Mechanisms Underlying the Enhanced Resolution of Atomic Force Microscopy with Functionalized Tips. *New J. Phys.* **2010**, *12*, 125020.
- (15) Hapala, P.; Kichin, G.; Wagner, C.; Tautz, F. S.; Temirov, R.; Jelínek, P. Mechanism of High-Resolution STM/AFM Imaging with Functionalized Tips. *Phys. Rev. B* **2014**, *90*, 085421.
- (16) Hapala, P.; Temirov, R.; Tautz, F. S.; Jelínek, P. Origin of High-Resolution IETS-STM Images of Organic Molecules with Functionalized Tips. *Phys. Rev. Lett.* **2014**, *113*, 226101.